


RESEARCH

Open Access



Umbilical mesenchymal stem cell-derived exosomes facilitate spinal cord functional recovery through the miR-199a-3p/145-5p-mediated NGF/TrkA signaling pathway in rats

Yang Wang^{1,2,3†}, Xunwei Lai^{1,2,3†}, Depeng Wu^{1,2,3†}, Bin Liu^{1,2,3}, Nanxiang Wang^{1,2,3} and Limin Rong^{1,2,3*} 

Abstract

Background: Although exosomes, as byproducts of human umbilical cord mesenchymal stem cells (hUC-MSCs), have been demonstrated to be an effective therapy for traumatic spinal cord injury (SCI), their mechanism of action remains unclear.

Methods: We designed and performed this study to determine whether exosomes attenuate the lesion size of SCI by ameliorating neuronal injury induced by a secondary inflammatory storm and promoting neurite outgrowth. We determined the absolute levels of all exosomal miRNAs and investigated the potential mechanisms of action of miR-199a-3p/145-5p in inducing neurite outgrowth in vivo and in vitro.

Results: miR-199a-3p/145-5p, which are relatively highly expressed miRNAs in exosomes, promoted PC12 cell differentiation suppressed by lipopolysaccharide (LPS) in vitro through modulation of the NGF/TrkA pathway. We also demonstrated that Cblb was a direct target of miR-199a-3p and that Cbl was a direct target of miR-145-5p. Cblb and Cbl gene knockdown resulted in significantly decreased TrkA ubiquitination levels, subsequently activating the NGF/TrkA downstream pathways Akt and Erk. Conversely, overexpression of Cblb and Cbl was associated with significantly increased TrkA ubiquitination level, subsequently inactivating the NGF/TrkA downstream pathways Akt and Erk. Western blot and coimmunoprecipitation assays confirmed the direct interaction between TrkA and Cblb and TrkA and Cbl. In an in vivo experiment, exosomal miR-199a-3p/145-5p was found to upregulate TrkA expression at the lesion site and also promote locomotor function in SCI rats.

(Continued on next page)

* Correspondence: ronglm@mail.sysu.edu.cn

[†]Yang Wang, Xunwei Lai and Depeng Wu contributed equally to this work.

¹Department of Spine Surgery, The Third Affiliated Hospital of Sun Yat-sen University, No. 600 Tianhe Road, Tianhe District, Guangzhou, Guangdong Province, China

²Guangdong Provincial Center for Engineering and Technology Research of Minimally Invasive Spine Surgery, No. 600 Tianhe Road, Tianhe District, Guangzhou, Guangdong Province, China

Full list of author information is available at the end of the article



© The Author(s). 2021 **Open Access** This article is licensed under a Creative Commons Attribution 4.0 International License, which permits use, sharing, adaptation, distribution and reproduction in any medium or format, as long as you give appropriate credit to the original author(s) and the source, provide a link to the Creative Commons licence, and indicate if changes were made. The images or other third party material in this article are included in the article's Creative Commons licence, unless indicated otherwise in a credit line to the material. If material is not included in the article's Creative Commons licence and your intended use is not permitted by statutory regulation or exceeds the permitted use, you will need to obtain permission directly from the copyright holder. To view a copy of this licence, visit <http://creativecommons.org/licenses/by/4.0/>. The Creative Commons Public Domain Dedication waiver (<http://creativecommons.org/publicdomain/zero/1.0/>) applies to the data made available in this article, unless otherwise stated in a credit line to the data.

(Continued from previous page)

Conclusions: In summary, our study showed that exosomes transferring miR-199a-3p/145-5p into neurons in SCI rats affected TrkA ubiquitination and promoted the NGF/TrkA signaling pathway, indicating that hUC-MSC-derived exosomes may be a promising treatment strategy for SCI.

Keywords: Exosomes, Umbilical cord mesenchymal stem cells, Spinal cord injury, microRNAs, TrkA ubiquitination, PC12 cells

Introduction

Acute traumatic spinal cord injury (SCI) has a prevalence rate of 10–83 per million [1] worldwide each year and usually results in devastating functional loss below the level of the injured spinal cord. The pathophysiology of SCI consists of primary mechanical injury and a subsequent cascade of inflammation, ischemia, and secretion of cytotoxic substances that aggravates SCI damage [2–4].

Neurons play a central role in transducing biological signals [5], but they fail to receive and send electrical and chemical signals following injury. Even though SCI patients achieve certain recovery of locomotion [6, 7], injured axons rarely reconnect to the same extent as axons in the normal spinal cord, and patient motor function never returns to normal [8]. A failed neuronal reconnection of two severed axons mainly occurs for the following reasons [8]: (a) loss of intrinsic outgrowth capacity of neurons, (b) deterioration of the microenvironment, and (c) inhibition of fibrous scar and glial scar formation. Therefore, promoting neurite outgrowth and improving the microenvironment of the remaining neurons should be essential for locomotor recovery in SCI patients.

TrkA, a critical member of the receptor tyrosine kinase (RTK) family composed of TrkA, TrkB, TrkC, and p⁷⁵NTR, can be phosphorylated and induced to form intracellular dimers in the structural domain by coupling with NGF, which subsequently initiates signaling cascades through phosphorylating Ras protein. Based on previous studies on the mechanism of action of NGF/TrkA, which is indispensable in the development and maturation of the nervous system [9]. Exosomes, important paracrine factors of stem cells, are nanosized particles with a diameter of 20 to 150 nm and consist of a lipid bilayer that encapsulates RNAs, DNAs, and soluble proteins [10, 11]. Currently, an increasing number of researchers have demonstrated that stem cell-derived exosomes share similar therapeutic effects as stem cells, such as inhibition of proinflammatory cytokines [12], inactivation of A1 astrocytes [13], and conversion of macrophages to the M2 phenotype [14].

Through preliminary experiment, we demonstrated that UC-MSC exosomes can help to stimulate the NGF/TrkA signaling pathway and promote the neuronal markers expression (NF-H, Neu-N, and β -tubulin-III)

inhibited by LPS in PC12 cells. Subsequently, we conducted this study to confirm the specific mechanisms of exosomes in inducing neurite outgrowth in vivo and in vitro and the efficacy of exosomes in treating SCI.

Materials and methods

Ethical statement

Ethical approval for the experiment was obtained from the Ethics Committee of the Third Affiliated Hospital of Sun Yat-sen University, China (Ethic number: IACUC-F3-19-0401). All experiments were performed following relevant laws and guidelines and the institutional guidelines of the Third Affiliated Hospital of Sun Yat-sen University. This article does not involve any human studies.

Animal experimental protocol

We purchased adult female Sprague-Dawley rats (6–7 weeks old), all specific pathogen-free (SPF), from Shanghai SLAC Laboratory Animal Co., Ltd. (Shanghai, China). All rats were housed in an SPF environment (temperature, 22 ± 1 °C; humidity, 65–70%) with free access to food and water, and five rats were assigned per cage. All animal experiments were approved by the animal ethics committee of the Third Affiliated Hospital of Sun Yat-sen University and in accordance with the guidelines included in the Guide for the Care and Use of Laboratory Animals published by the National Institutes of Health (Eighth Edition). In total, seventy-six rats were sacrificed by CO₂ suffocation (detailed animal information is provided in Additional file 1).

Exosome purification and characterization

Exosomes were isolated from the supernatants of passage 5 hUC-MSCs according to the Total Exosome Extraction Reagent (Invitrogen, Carlsbad, California, USA) instructions. Before being subjected to transmission electron microscopy (TEM; Tokyo, Japan) and the qNano nanoparticle analysis system (Izon, Christchurch, New Zealand), exosomes in suspension were filtered using a 220-nm filter and stained with 3% aqueous phosphotungstic acid. Exosomes were lysed with radioimmunoprecipitation assay (RIPA) buffer (Beyotime, Shanghai, China) supplemented with a protease and phosphatase-inhibitor cocktail (CST, Boston, MA, USA). The protein concentration of exosomes was quantified using the

BCA Protein Assay Kit (Thermo Fisher, Boston, MA, USA). Primary antibodies against CD63 (Abcam, Cambridge, UK), CD9 (Abcam, Cambridge, UK), and β -actin (CST, Boston, MA, USA) were used to characterize exosomes (detailed methods and materials are provided in Additional file 2).

Statistical analysis

Statistical analysis was performed, and graphs were generated by using Graph Pad Prism 8.0 (San Diego, CA, USA). All data are presented as the mean \pm standard

deviation (SD) and the range from min to max, and differences were analyzed using one-way analysis of variance (one-way ANOVA). $P < 0.05$ was considered statistically significant.

Results

Exosomal miRNA profile analyzed by absolute quantitative sequencing

We obtained hUC-MSCs from Guangzhou Selera Stem Cell Technology Co., Ltd., and the cells that presented a long spindle shape were identified by flow cytometry. Stem cell markers (CD73, CD90, CD105) (Fig. 1a) were

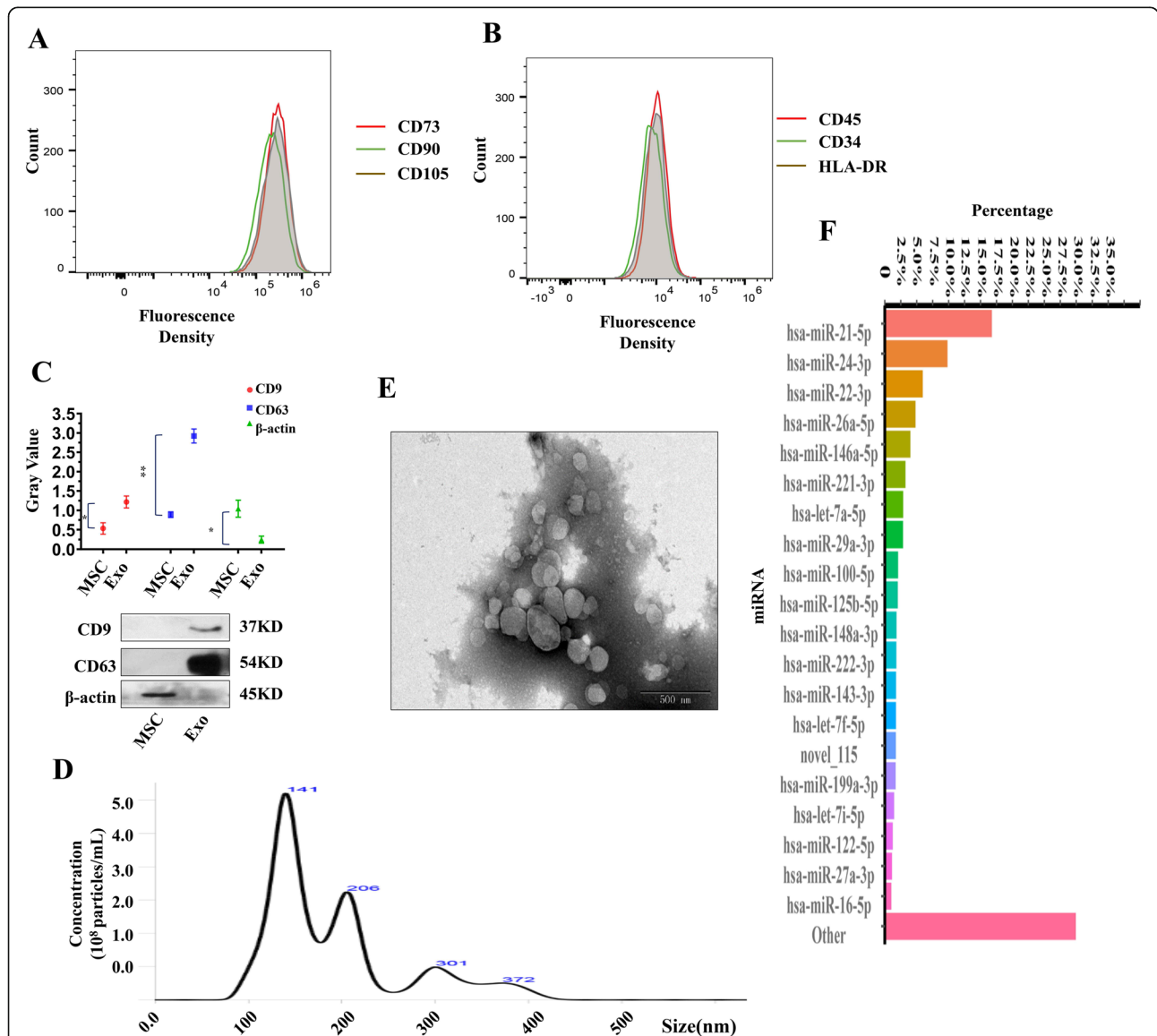


Fig. 1 MSC and MSC-Exo characterization and exosomal miRNA profiles. hUC-MSCs were characterized by CD73, CD90, CD105 (a), CD45, CD34, and HLA-DR (b) expression by using flow cytometry. c Representative images and quantitative analysis of western blots to assess CD9, CD63, and β -actin expression in MSCs and MSC-Exo ($n = 3$). Data are represented as mean \pm SD. d The morphology of exosomes detected by transmission electron microscopy ($n = 3$). Scale bar = 500 nm. e The diameters and concentrations of exosomes analyzed by the nanoparticle tracking method. f Top 20 miRNAs expressed in MSC-Exo. MSC mesenchymal stem cell, MSC-Exo MSC-derived exosomes. * $p < 0.05$; ** $p < 0.01$

highly expressed, while non-stem cell markers (CD45, CD34, HLA-DR) (Fig. 1b) were expressed at extremely low levels on the cell surface. Then, we purified exosomes from the culture supernatants of MSCs by the Total Cell Exosome Extraction Kit. Analysis of the morphology and surface markers confirmed that the obtained pellet were exosomes. First, CD9 and CD63 were detected in these particles, which did not express β -actin (Fig. 1c). Nanoparticle tracking analysis (NTA) revealed the concentration and size of the particles ranging from 30 to 150 nm (Fig. 1d). Furthermore, a typical cup-shaped morphology of these nanoparticles was observed by transmission electron microscopy (TEM) (Fig. 1e).

miRNAs are the most abundant nucleic acids in MSC-derived exosomes (MSC-Exo) and play important roles in regulating cell activities. To obtain a better understanding of the exosomal miRNA profile, we performed small RNA absolute quantitative sequencing (see Additional file 6) of MSC-Exo, and the results are deposited in the GEO database of NCBI (GEO database: GSE 159814). The sequence results are provided in Additional file 6. Small RNA sequencing identified approximately 990 miRNAs in MSC-Exo. Further analysis showed a linear relationship between log-transformed standard deviation (SD) and transcripts per million (TPM) values (see Additional file 7A).

The top 20 miRNAs (plus miR-145-5p) and the miRNA-target network are provided (Fig. 1f, see Additional file 7B). miR-199a-3p (Fig. 1f) and miR-145-5p [15] were very abundant in MSC-Exo. We presumed that miR-199a-3p/145-5p regulate the TrkA turnover, because we found the direct relationship between miR-199a-3p and Cblb, miR-145-5p, and Cbl through on-line bioinformatic analysis (see Additional file 7B). As for Cbl and Cblb, they are critical enzyme in the modulation of TrkA degradation by lysosome. Subsequently, we examined how the exosomal miR-199a-3p/145-5p impact the neuronal differentiation through the regulation of Cblb and Cbl genes.

miR-199a-3p/145-5p acted as critical effectors in MSC-Exo-mediated neuronal differentiation of PC12 cells in vitro and in vivo

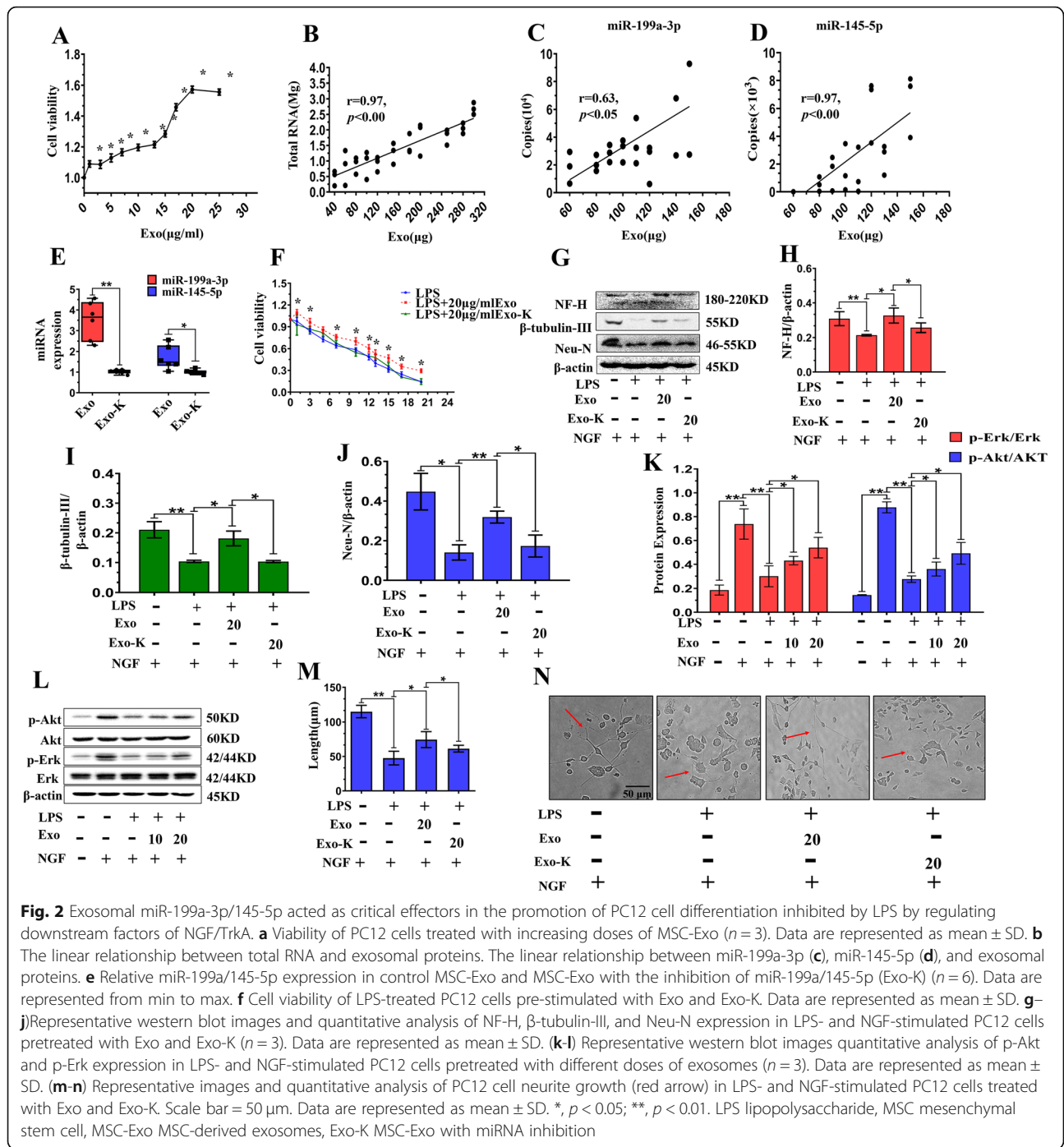
To investigate the synergistic effects of miR-199a-3p/145-5p in exosomes, we cotransfected MSCs with miR-199a-3p/145-5p antisense RNAs and then purified exosomes from the culture supernatants of non-treated MSCs (Exo) and cotransfected MSCs (Exo-K). First, we confirmed that PC12 cell viability increased dose-dependently with exosome concentrations (0, 1, 3, 5, 7, 10, 13, 15, 17, 20, 25 μ g/ml), and 20 μ g/ml was the most effective concentration in PC12 cells (1.6 times higher viability than that of the control) (Fig. 2a). The successful endocytosis of MSC-Exo by PC12 cells was confirmed by PKH26-labeled

exosomes (See Additional file 8A). Subsequently, we confirmed that the total RNA content was positively associated with the amount of exosomal proteins (40, 60, 80, 100, 120, 150, 180, 200, 250, 280, 300 μ g) quantified by BCA assay (Fig. 2b). Moreover, the levels of miR-199a-3p (Fig. 2c) and miR-145-5p (Fig. 2d) showed a linear relationship with the amount of exosomal proteins.

Interestingly, we found different miR-199a-3p/145-5p expression profiles between primary neurons, astrocytes, endothelial cells, and meningeal fibroblasts. Among these four types of primary cells, neurons had the highest levels of miR-145-5p and the lowest levels miR-199a-3p (see Additional file 8B). All primary cells were isolated from rats (see Additional file 8C). Moreover, through QRT-PCR analysis, we also discovered more miR-199a-3p transcripts than miR-145-5p transcripts in PC12 cells (See Additional file 8D).

Then, miR-199a-3p/145-5p expression was successfully inhibited in MSC-Exo (Exo-K) (Fig. 2e). Experiments were conducted to determine the optimal concentration of LPS, and the results demonstrated that the LPS concentration (0, 1, 3, 5, 7, 10, 11, 13, 15, 17, 20 μ g/ml) had a dose-dependent effect on PC12 cell viability; 11 μ g/ml LPS was selected to establish an injury model in PC12 cells (Fig. 2f). Furthermore, when PC12 cells were pretreated with 20 μ g/ml MSC-Exo, cell viability was rescued (Fig. 2f). However, 20 μ g/ml Exo-K could not rescue PC12 cell viability (Fig. 2f).

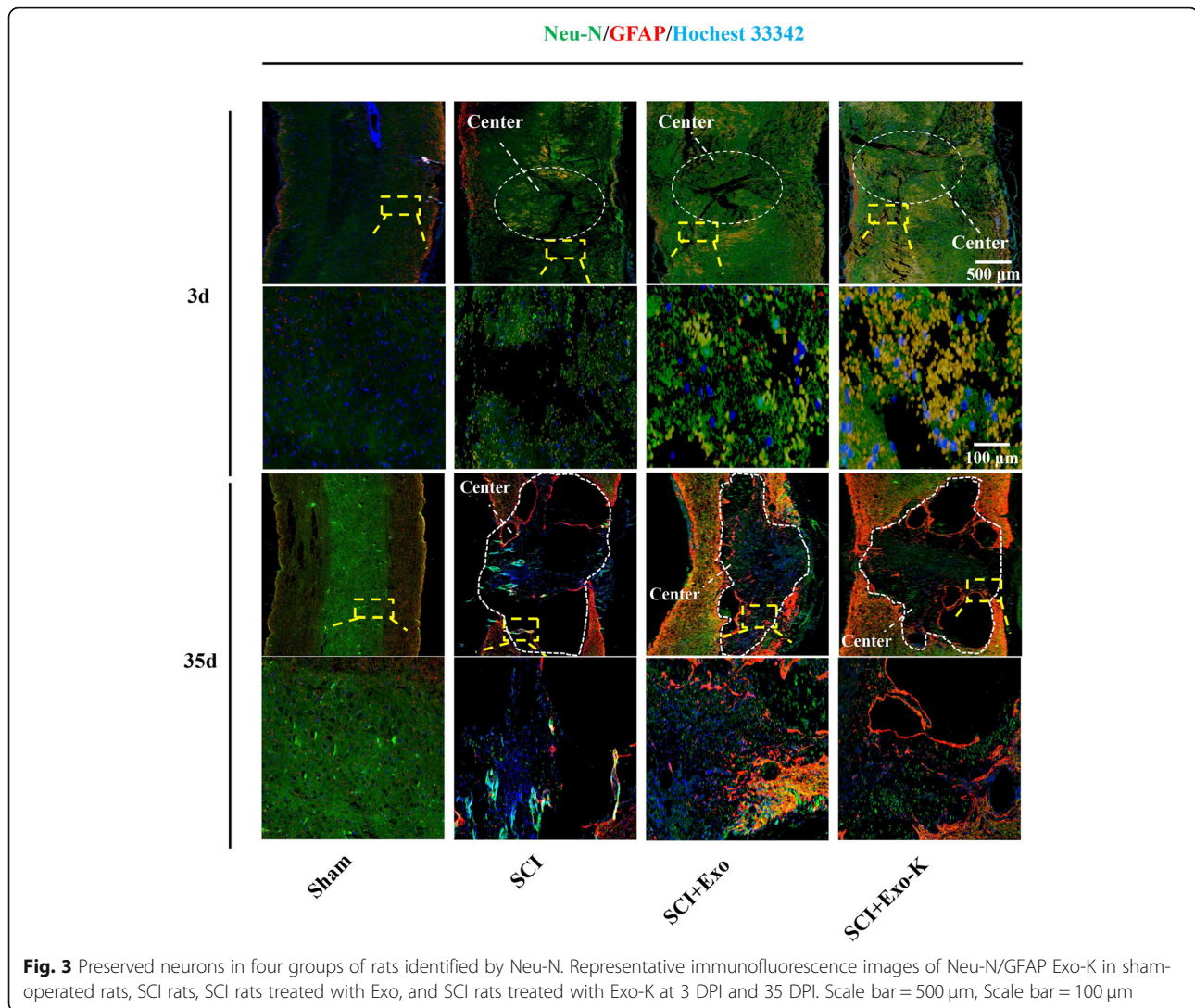
Furthermore, we pretreated PC12 cells, which were subsequently stimulated by NGF and LPS, with MSC-Exo to investigate whether exosomal miR-199a-3p/145-5p were indispensable in NGF-induced PC12 differentiation. Our results showed that neuronal marker expression (NF-H, β -tubulin-III, Neu-N) suppressed by LPS could be upregulated by Exo; however, this protective effect was partially abolished by knockdown of miR-199a-3p/145-5p in MSC-Exo (Fig. 2g–i). The results also showed that the downregulation of p-Akt and p-Erk induced by LPS was also reversed by increasing doses of MSC-Exo (Fig. 2k, l). Moreover, the inhibition of PC12 neurite outgrowth induced by LPS, which was partially reversed by MSC-Exo, was closely related to exosomal miR-199a-3p/145-5p expression (Fig. 2m, n). More importantly, we observed that neurons were greatly preserved at 3- and 35-days post injury (DPI) as demonstrated by Neu-N staining (Fig. 3). The compromised effect of Exo-K on the promotion of neurite outgrowth, which was inhibited by LPS, was also observed in primary neurons in vitro (see Additional file 9A). Thus, the presence of miR-199a-3p/145-5p recapitulated the neuroprotective effects of MSC-Exo, while miR-199a-3p/145-5p knockdown suppressed these effects. Moreover, we found that miR-199a-3p/145-5p levels in MSC-Exo



were correlated with increased endothelial cell migration and tube formation abilities, which were suppressed by LPS (see Additional file 9B-E), while these effects were compromised by MSC-Exo-K. This finding may explain why exosomes are often administered in the early stage of SCI, as the blood supply is potentially impacted as well. In summary, miR-199a-3p/145-5p participated in MSC-Exo-mediated neurite outgrowth in vitro and in vivo.

miR-199a-3p/145-5p promoted PC12 cell differentiation by regulating downstream factors of NGF/TrkA

To investigate whether exogenous miR-199a-3p/145-5p showed similar positive effects on neurite outgrowth, we pretransfected miR-199a-3p/145-5p mimics into PC12 cells before treatment with LPS or NGF. The results revealed that LPS dramatically reduced neuronal marker (NF-H, β -tubulin-III, Neu-N) expression at the protein



and mRNA levels, which was rescued by miR-199a-3p/145-5p mimics in a dose-dependent manner (Fig. 4a, b; Fig. 5a, b). The significant suppression of p-Akt and p-Erk by LPS, which could be highly activated by NGF, was also partially promoted by miR-199a-3p/145-5p mimics in a dose-dependent manner (Fig. 4c, d; Fig. 5c, d). Furthermore, increasing doses of miR-199a-3p/145-5p mimics also led to dose-dependent promotion of LPS-stimulated PC12 neurite outgrowth, and neuronal markers (NF-H, β -tubulin-III, Neu-N) were examined and visualized by confocal microscopy (Fig. 4e, f; Fig. 5e, f). This observation suggests that miR-199a-3p/145-5p are involved in the NGF/TrkA pathway and PC12 cell differentiation.

miR-199a-3p and miR-145-5p targeted the Cblb and Cbl genes, respectively

Through bioinformatics prediction, we hypothesized that Cblb and Cbl were direct targets of miR-199a-3p and

miR-145-5p, respectively (Fig. 6a, b). To investigate whether miR-199a-3p regulated Cblb gene expression at the transcriptional or posttranscriptional level, we transfected both miR-199a-3p/145-5p mimics and inhibitors into PC12 cells. Western blotting and QRT-PCR showed that Cblb, and Cbl protein and mRNA expressions decreased with increasing doses of the mimics and increased with increasing doses of the inhibitors (Fig. 6c–e). These results suggested that miR-199a-3p/145-5p suppressed Cblb and Cbl expression in PC12 cells at the transcriptional and posttranscriptional levels.

Furthermore, we cloned the two predicted wild-type binding sites (WT-1/-2) and the mutant sites into plasmids and cotransfected the pGL3-reporter and pRL-TK vector with miRNA mimics or inhibitors into HEK293 cells. A previous study predicted a relationship between miR-199a-3p and Cblb, while our results demonstrated a direct interaction between them. Significant changes in relative luciferase activity in HEK293 cells transfected

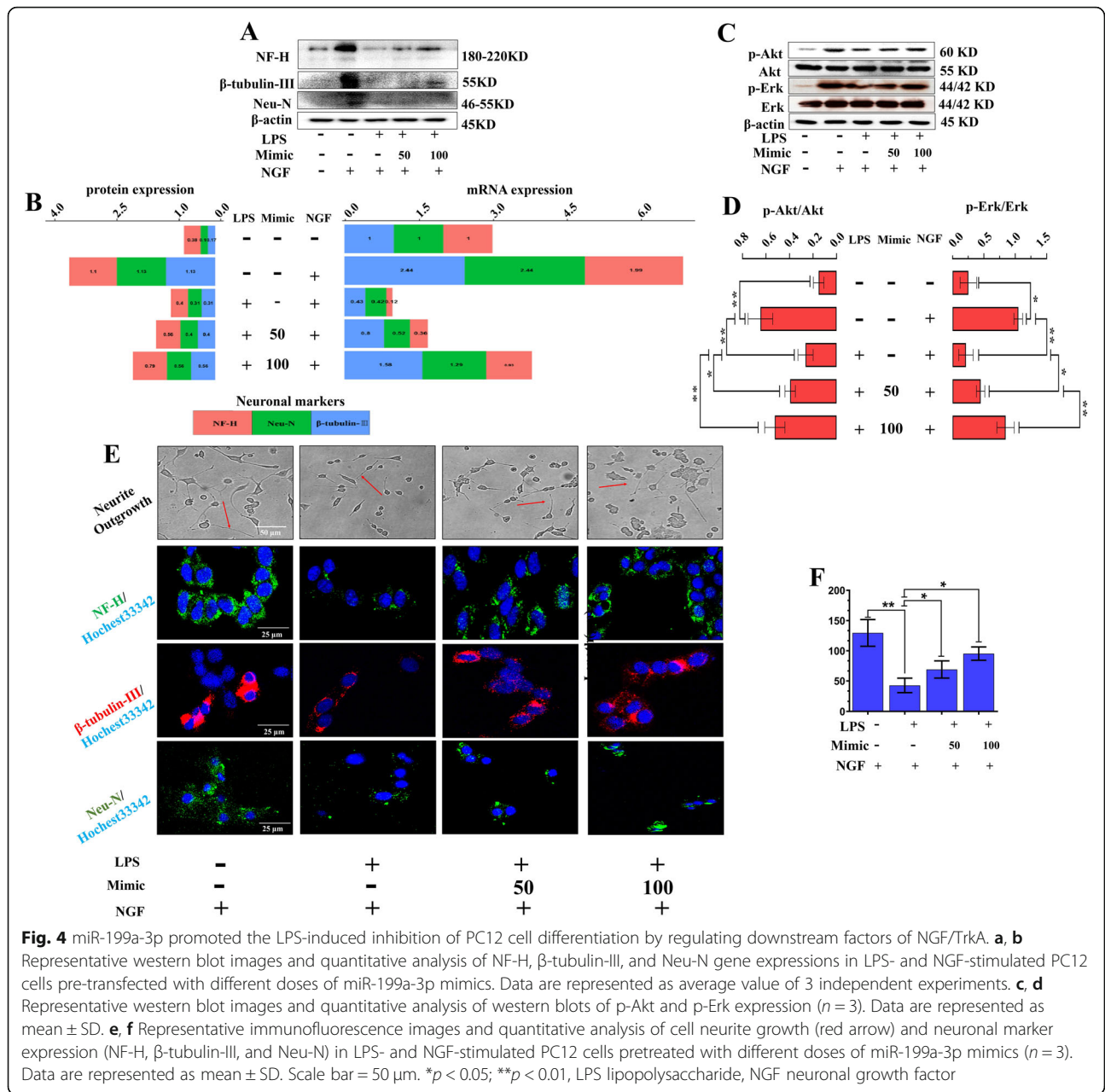


Fig. 4 miR-199a-3p promoted the LPS-induced inhibition of PC12 cell differentiation by regulating downstream factors of NGF/TrkA. **a, b** Representative western blot images and quantitative analysis of NF-H, β-tubulin-III, and Neu-N gene expressions in LPS- and NGF-stimulated PC12 cells pre-transfected with different doses of miR-199a-3p mimics. Data are represented as average value of 3 independent experiments. **c, d** Representative western blot images and quantitative analysis of western blots of p-Akt and p-Erk expression (n = 3). Data are represented as mean ± SD. **e, f** Representative immunofluorescence images and quantitative analysis of cell neurite growth (red arrow) and neuronal marker expression (NF-H, β-tubulin-III, and Neu-N) in LPS- and NGF-stimulated PC12 cells pretreated with different doses of miR-199a-3p mimics (n = 3). Data are represented as mean ± SD. Scale bar = 50 μm. *p < 0.05; **p < 0.01, LPS lipopolysaccharide, NGF neuronal growth factor

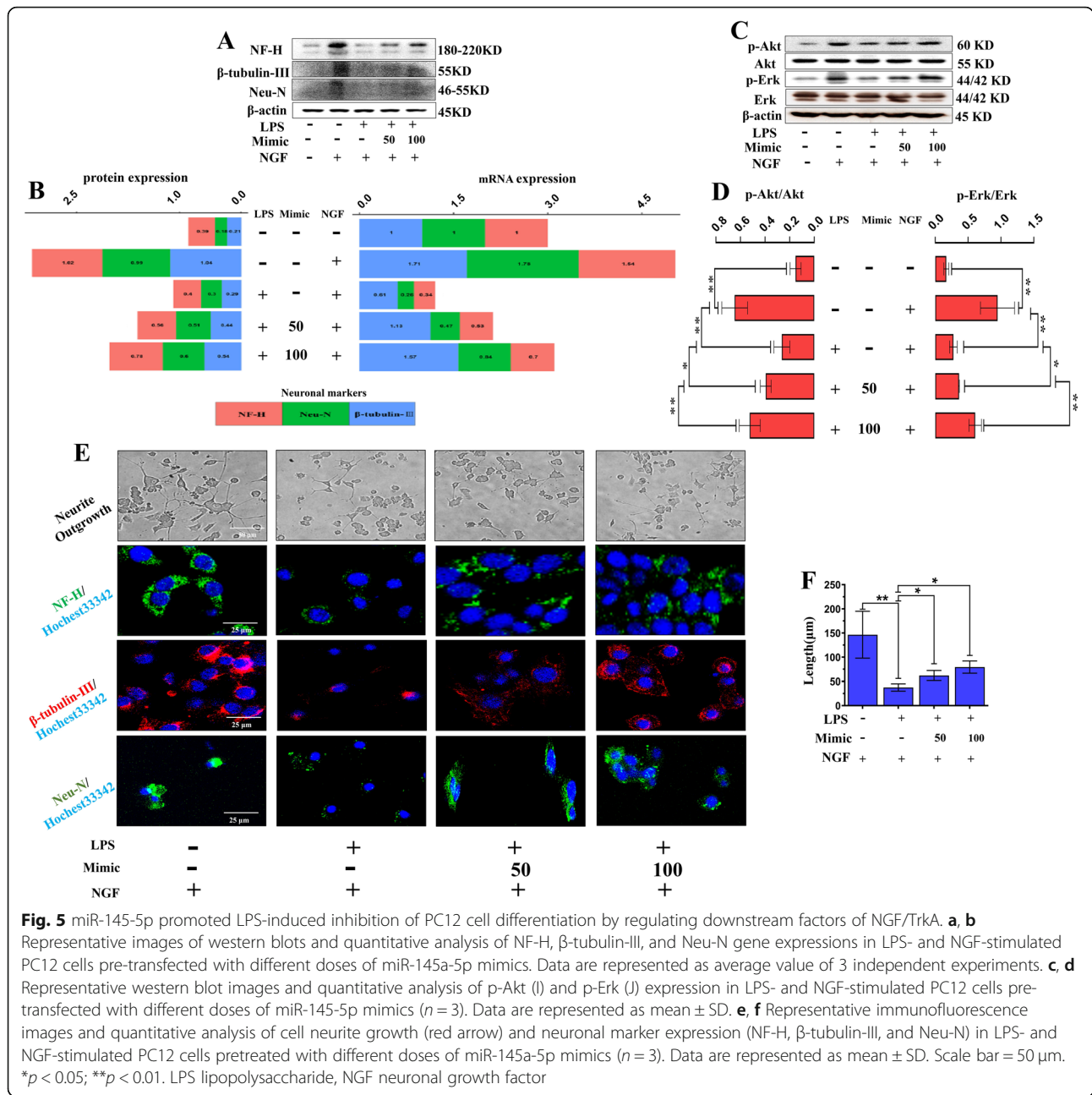
with scramble sequence (Si NC group) were not observed, while decreased luciferase activity along with increasing doses of the miR-199a-3p mimic was determined (Fig. 6f, g). Increased luciferase activity in HEK293 cells was also observed when cells were transfected with 150 nm miR-199a-3p mimics (Fig. 6f, g). Regardless of whether the cells were transfected with miR-199a-3p mimics or inhibitors, the luciferase activity of HEK293 cells transfected with a vector carrying mutant sites was not affected (Fig. 6f, g).

Regardless of whether the cells were transfected with miR-145-3p mimics or inhibitors, the luciferase activity of HEK293 cells transfected with a vector carrying the

mutant site was not significantly changed (Fig. 6h). The scramble control did not influence luciferase activity in HEK293 cells. These results suggested that miR-199a-3p/145-5p suppressed Cblb and Cbl expression via direct binding to their predicted mRNA seed regions.

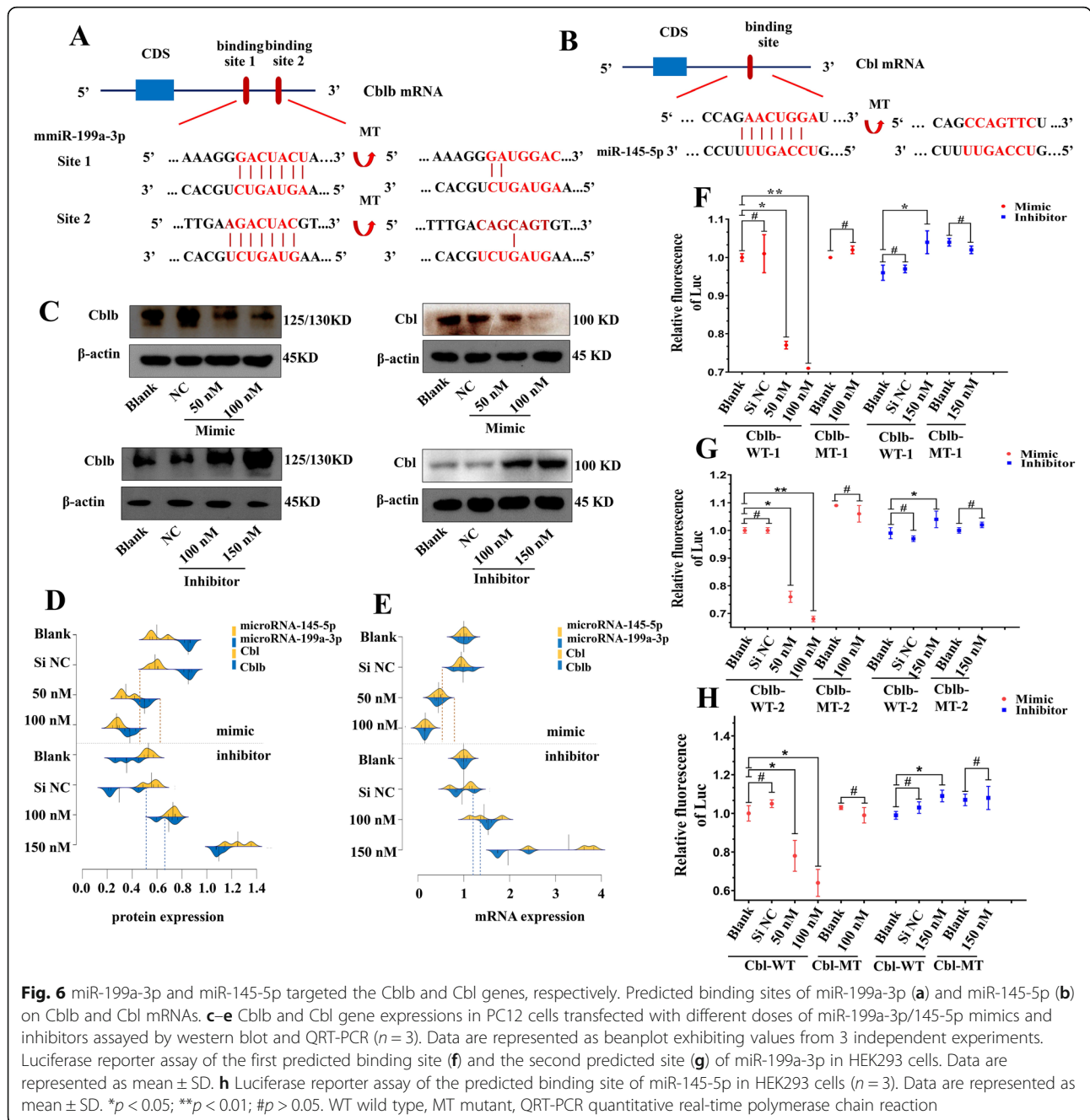
Cblb and Cbl regulated the NGF/TrkA pathway through modulation of TrkA ubiquitination

To further explore how Cblb and Cbl interact with the NGF/TrkA pathway, we knocked down or overexpressed these two genes in PC12 cells. First, we designed three siRNAs against the Cblb and Cbl genes, two of which (Si



#1 and Si #2) were more effective in suppressing Cblb and Cbl mRNA expression (see Additional file 10A-B; 10D-E). When Cblb and Cbl were knocked down by the siRNAs, total ubiquitinated proteins in PC12 cells were greatly reduced; however, a marked increase in TrkA was observed compared with that in nontreated cells (Fig. 7a, b). Single knockdown of Cblb or Cbl caused up-regulation of p-Erk and p-Akt, and NGF activated p-Erk and p-Akt (Fig. 7c, d), subsequently promoting NGF-induced neurite outgrowth in PC12 cells (see Additional file 10C; 10F).

Then, we successfully upregulated Cblb and Cbl expression in PC12 cells (see Additional file 11). Overexpression of Cblb and Cbl led to higher ubiquitination levels of total proteins and lower expression of TrkA (Fig. 7e, f). NGF stimulation accelerated the degradation process of TrkA when Cblb and Cbl were overexpressed, but this process was inhibited by the proteasome inhibitor MG-132 (Fig. 7e, f). We also found that NGF-activated p-Erk and p-Akt were further upregulated in Cblb- and Cbl-overexpressing cells by the protease inhibitor MG-132 (Fig. 7g, h). More

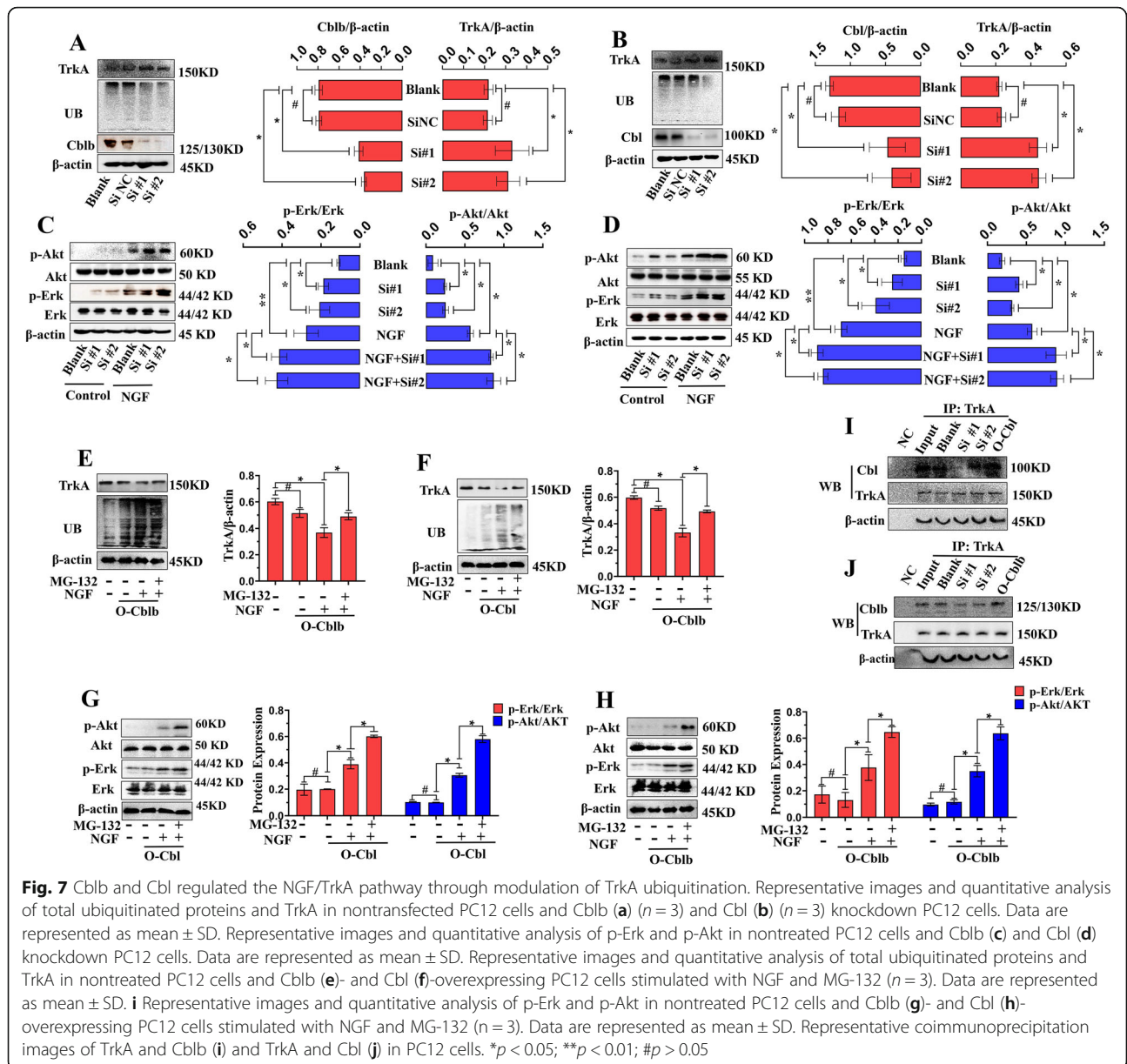


importantly, we pulled down Cblb and Cbl proteins in PC12 cells with knockdown and overexpression of Cblb and Cbl by using a primary antibody against TrkA, further confirming the direct interaction between Cblb and TrkA (Fig. 7i, j).

Exosomal miR-199a-3p/145-5p alleviated damage to the lesion site and facilitated locomotor function in SCI rats

In vivo, we injected the rats with PBS, Exo, and Exo-K via the tail vein. The high expression of miR-199a-3p and miR-145-5p in rats receiving Exo injection was

partially downregulated in rats receiving Exo-K injection, which implied the successful delivery of the miRNAs by exosomes (Fig. 8a). Further, track of PKH26-labeled exosomes by immunofluorescence in vivo proved this point (see Additional file 12). We also observed that the increase in TrkA in rats receiving Exo injection was partly downregulated in rats receiving Exo-K injection at 3 DPI (Fig. 8b). Exo injection exerted an antiapoptotic effect on the lesion site, while this effect was abrogated with the inhibition of miR-199a-3p/145-5p (Fig. 8c, d). Decreased inflammatory levels in vivo were also partially



attributed to exosomal miR-199a-3p/145-5p levels (see Additional file 13).

The Basso, Beattie and Bresnahan (BBB) scale was used to assess the locomotor function of the hindlimbs of rats, and the values were recorded from onset to 35 DPI. Strongly impaired locomotor function of the hindlimbs of rats was observed on the 1st DPI, and significant improvement was detected on the 7th DPI (Fig. 8e). Hematoxylin-eosin (HE) staining showed that the damage at the lesion site of SCI rats was smaller than that of SCI + Exo rats. Interestingly, this protective effect was partially suppressed when miR-199a-3p/145-5p were inhibited in MSC-Exo (Fig. 8f, g). We further detected spinal cord damage in vivo, and the MRI results

indicated that MSC-Exo greatly decreased the lesion size of the injured spinal cord, while Exo-K exerted weaker protective effects on the damaged spinal cord (Fig. 8h). These data indicated the pivotal roles of miR-199a-3p/145-5p in MSC-Exo-mediated treatment of SCI in vivo (Fig. 9). Cbl and Cbl inhibition by exosomal miR-199a-3p/145-5p emphasized the neuroprotective effect of MSC-Exo.

Discussion

miRNAs, noncoding RNAs of approximately 22 nucleotides, depending on the exosomal origins, are markedly enriched in exosomes and target mRNAs by binding to

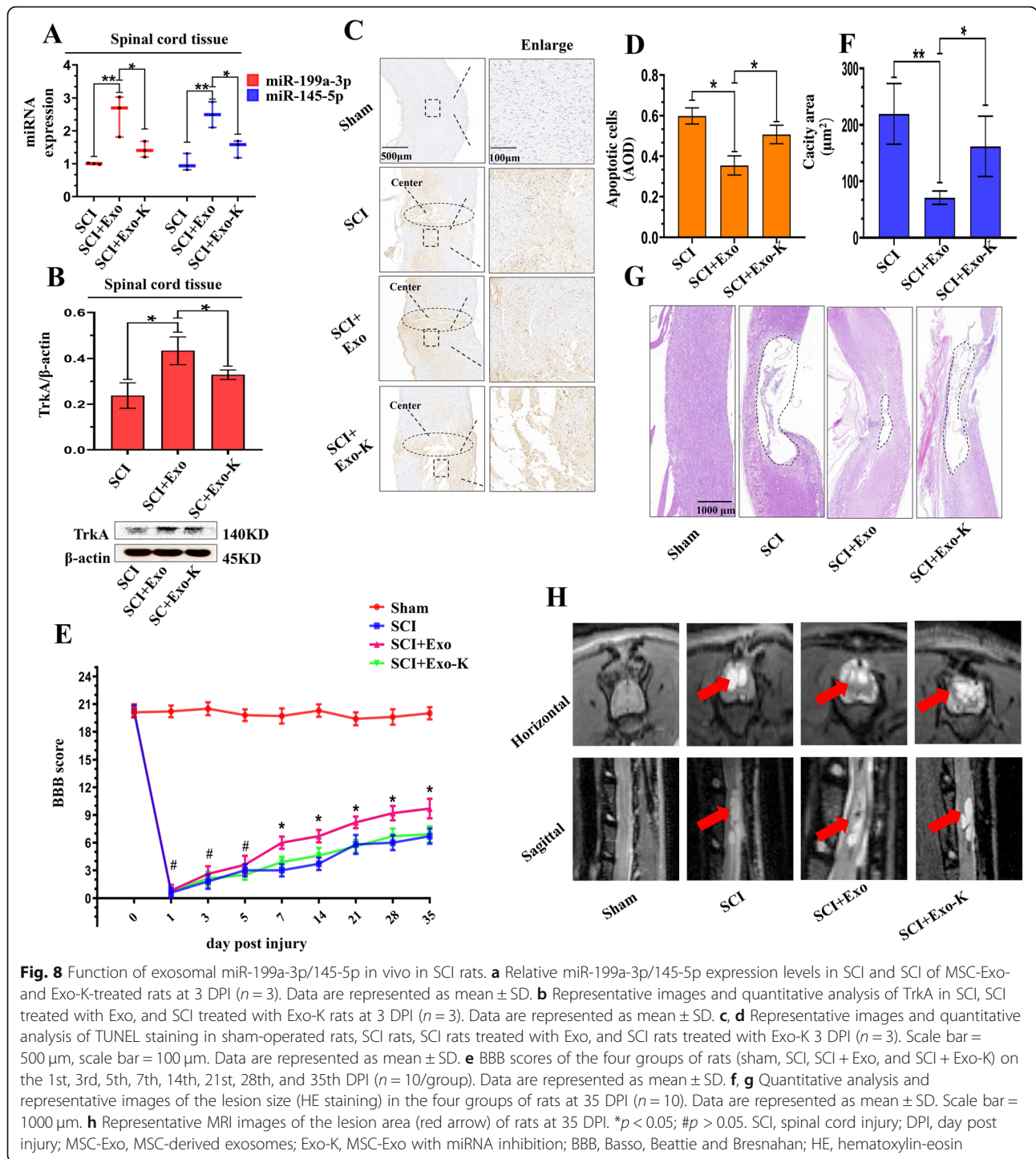
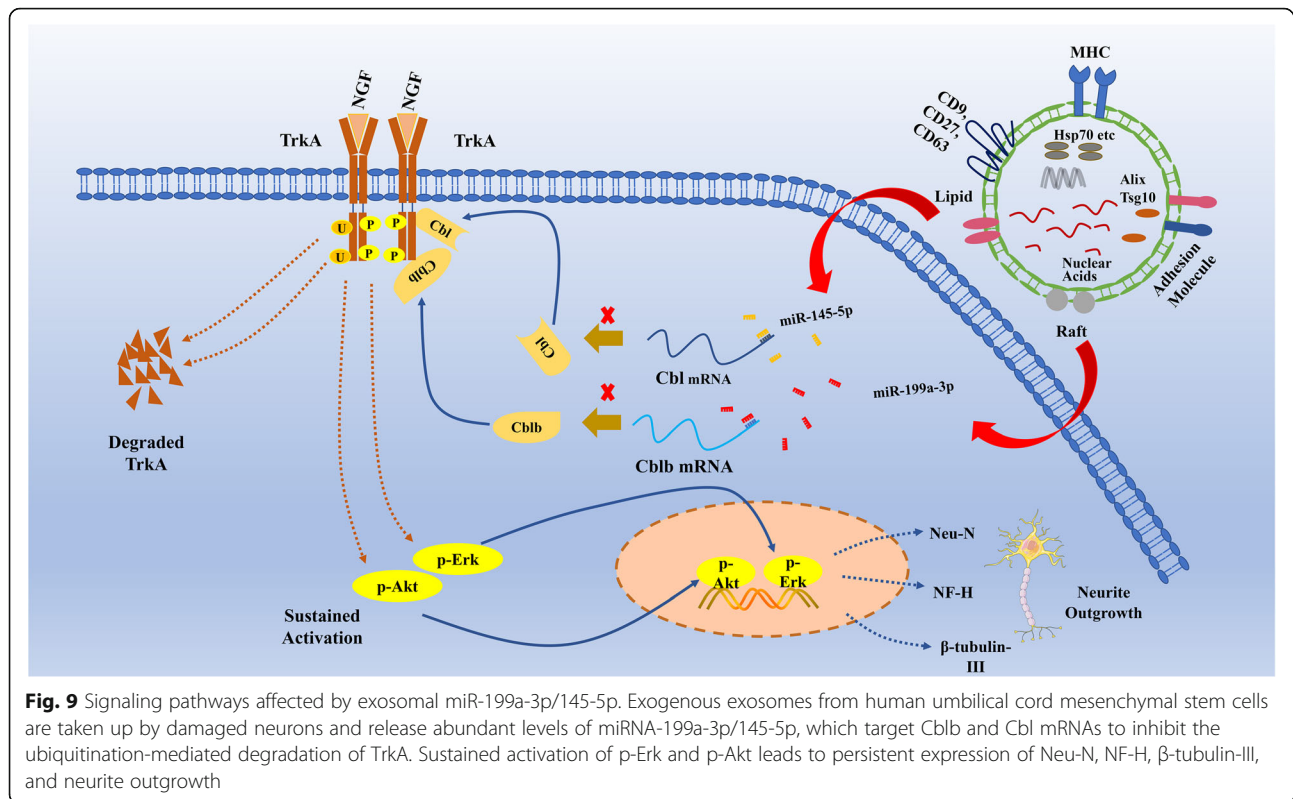


Fig. 8 Function of exosomal miR-199a-3p/145-5p in vivo in SCI rats. **a** Relative miR-199a-3p/145-5p expression levels in SCI and SCI of MSC-Exo and Exo-K-treated rats at 3 DPI ($n = 3$). Data are represented as mean \pm SD. **b** Representative images and quantitative analysis of TrkA in SCI, SCI treated with Exo, and SCI treated with Exo-K rats at 3 DPI ($n = 3$). Data are represented as mean \pm SD. **c, d** Representative images and quantitative analysis of TUNEL staining in sham-operated rats, SCI rats, SCI rats treated with Exo, and SCI rats treated with Exo-K 3 DPI ($n = 3$). Scale bar = 500 μ m, scale bar = 100 μ m. Data are represented as mean \pm SD. **e** BBB scores of the four groups of rats (sham, SCI, SCI + Exo, and SCI + Exo-K) on the 1st, 3rd, 5th, 7th, 14th, 21st, 28th, and 35th DPI ($n = 10$ /group). Data are represented as mean \pm SD. **f, g** Quantitative analysis and representative images of the lesion size (HE staining) in the four groups of rats at 35 DPI ($n = 10$). Data are represented as mean \pm SD. Scale bar = 1000 μ m. **h** Representative MRI images of the lesion area (red arrow) of rats at 35 DPI ($n = 10$). $*p < 0.05$; $\#p > 0.05$. SCI, spinal cord injury; DPI, day post injury; MSC-Exo, MSC-derived exosomes; Exo-K, MSC-Exo with miRNA inhibition; BBB, Basso, Beattie and Bresnahan; HE, hematoxylin-eosin

their 3' UTRs [16, 17]. The hUC-MSC-derived exosomal miRNA expression profiles first identified by Fang using QRT-PCR (miR-21, -23a, -125b, -145) [18] and then quantified by us using absolute quantitative sequencing shared similar results. Cargo miRNAs, as the most abundant nucleotides in exosomes, are receiving increasing attention from researchers, mainly owing to the

improved understanding of miRNAs and advances in the techniques used to investigate miRNAs.

Findings showing attenuated central inflammation in rats through detection of IL-1, IL-6, and TNF- α ; upregulation of proinflammatory cytokines (IL-4, IL-10); and reduction in apoptotic neurons in the early process of exosomal treatment [14] were consistent



with our results. Improvement of the microenvironment at the lesion site enhanced neurite outgrowth-related p-Akt/p-Erk pathway activation by NGF in PC12 cells and decreased secondary apoptosis of neurons. However, there is less evidence that exosomal miRNAs are involved in the protection of neurons at the early stage of SCI, and the underlying mechanism remains unclear. The injury model of PC12 cells was established by using LPS instead of other inflammatory cytokines as previously reported [19] because both LPS model and other inflammatory models truly reflect the damaged status of neurons under inflammation [20, 21]. Through knockdown of miR-199a-3p/145-5p in exosomes, we demonstrated the crucial role of miR-199a-3p/145-5p in the neuronal differentiation promoted by exosomes. Furtherly, we predicted that Cblb and Cbl genes are targeted by miR-199a-3p and miR-145-5p.

The protooncogenes Cbl and Cblb have been suggested to have a negative effect on RTKs, and the regulation of both genes is analogous to that of T cell receptor and epidermal growth factor (EGFR) [22–25]. As demonstrated for RTKs, E3 ubiquitin ligases such as NEDD4-2, tumor necrosis factor receptor-associated factor 6 (TRAF6), Cbl, and Cblb facilitate TrkA ubiquitination, internalization, and turnover [26–28]. Ubiquitins

(Cbl and Cblb) are conjugated onto TrkA along with the onset of self-phosphorylation of intracellular peptide fragments of TrkA, which can be suppressed by exosomal miR-199a-3p/145-5p in vivo and in vitro. Through an in vitro study, we determined that the Cbl mRNA 3' UTR was the target of miR-145-5p and that the Cblb mRNA 3' UTR was the target of miR-199a-3p. The predicted binding site of Cbl mRNA for miR-145-5p is first reported and proved by us; interestingly, the predicted binding site of Cblb mRNA for miR-199a-3p was previously reported but not examined in RAW264.7 cells by Rong [29].

In the absence of the Cbl and Cblb genes, an activation of the p-Akt/p-Erk pathways and increased neurite growth stimulated by NGF were observed. However, both the p-Akt/p-Erk pathways were soon downregulated, which was associated with rapid degradation of TrkA in response to NGF stimulation and the overexpression of Cblb and Cbl genes. Similar to Takahashi's results [27–30], our co-IP data showed that TrkA ubiquitination and degradation were statistically affected by Cbl, but the domain of TrkA required for ubiquitination by Cbl remains unclear. The mechanisms of the TrkA-Cblb interaction may involve the TKB domain (an SH2-like domain) promoting the binding of phosphorylated tyrosine on activated TrkA and Src homology 2 adapter

protein 2 (SH2B2, also known as APS) [31]. We showed from two aspects that the levels of Cblb and Cbl proteins, which could be clearly reduced by exosomal miRNAs, were associated with neurite outgrowth in PC12 cells and were potential influencing factors for SCI by affecting the turnover and/or activation of TrkA and maintaining sustained activation of p-Erk/p-Akt and neurite outgrowth. Intriguingly, this theory is potentially suitable for other E3 ubiquitin ligases, other Trk members regulating neurite outgrowth, and these E3 ubiquitin ligases are underlying targets of exosomes that are enriched for regulatory noncoding RNAs. Furthermore, knockdown of both miRNAs in exosomes directly led to lower expression of TrkA in vivo and impaired neurological function in SCI rats, which emphasized the effects of miR-199a-3p/145-5p in vivo.

Even though multiple drugs, such as nonsteroidal anti-inflammatory drugs (NSAIDs), anti-CD11d antibodies, minocycline, progesterone, estrogen, riluzole, polyethylene glycol (PEG), astatin and inosine, are already used in human clinical applications, satisfying outcomes are rarely obtained [32]. The use of exosomes in treating SCI is mainly due to the therapeutic effect of stem cells, which is thought to be a result of paracrine mechanisms, and an increasing number of researchers speculate that exosomes are a promising next-generation cell-free agent. However, rigorous assessment of their efficacy and safety and detailed mechanisms of action are urgently needed before or in conjunction with clinical application.

Conclusions

In summary, miR-199a-3p/145-5p derived from hUC-MSCs could promote locomotor functional recovery of SCI rats potentially by targeting the Cblb and Cbl genes, which resulted in modulation of the turnover and/or activation of TrkA. Furthermore, exosomes tended to promote neurite outgrowth by decreasing the inflammatory level at the lesion site of the spinal cord, creating a favorable environment for neurite outgrowth.

Supplementary Information

The online version contains supplementary material available at <https://doi.org/10.1186/s13287-021-02148-5>.

Additional file 1. Animal protocol.

Additional file 2. Supplementary methods and materials.

Additional file 3. siRNA and miRNA sequences.

Additional file 4. Coding Sequence of Cbl and Cblb Genes.

Additional file 5. Primers of target genes.

Additional file 6. Outcome of miRNA sequencing.

Additional file 7. Bioinformatic analysis of miRNAs. (A) The linear relationship between IgSD-2 and IgTPM. (B) Predicted target genes of the top 20 miRNAs (plus miR-145-5p) in miRanda. TPM, transcripts per million; SD, standard difference.

Additional file 8. Images of MSC-Exo taken up by PC12 cells and miR-199a-3p and miR-145-5p expression profiles in different cells. (A) Representative images of MSC-Exo taken up by PC12 cells. Scale bar=25 μ m. (B) The morphology of primary neurons, astrocytes, endothelial cells and meningeal fibroblasts visualized by an inverted fluorescence microscope. Scale bar=50 μ m. MSC-Exo, MSC-derived exosomes; QRT-PCR, quantitative real-time polymerase chain reaction.

Additional file 9. The effects of exosomal miR-199a-3p/miR-145-5p on endothelial cell migration, tube formation, and neurite outgrowth of primary neurons in vitro. (A) Representative images of neurite outgrowth (red arrow) in LPS-stimulated primary neurons pretreated with Exo and Exo-K. Scale bar=50 μ m. (B) Representative images of cell migration in LPS-stimulated endothelial cells pretreated with Exo and Exo-K (n=3). Scale bar=50 μ m. (C) Representative images of tube formation in LPS-stimulated endothelial cells pretreated with Exo and Exo-K (n=3). Scale bar=50 μ m. (D) Quantitative analysis of migrated cells in (B) and (E) the length of the tubes in (C). Data are represented as mean \pm SD. LPS, lipopolysaccharide; MSC, mesenchymal stem cell; MSC-Exo, MSC-derived exosomes; Exo-K, MSC-Exo with the inhibition of miRNAs.

Additional file 10. Knockdown of Cblb and Cbl increased NGF-induced neurite outgrowth in PC12 cells. Cblb mRNA level in nontransfected PC12 cells and PC12 cells transfected with scramble sequence, Cblb siRNA #1, siRNA #2, and siRNA #3 as detected by QRT-PCR (A). Data are represented as mean \pm SD. Quantitative analysis (B) and representative images (C) of cell neurite growth in NGF-stimulated PC12 cells transfected with scramble sequence, Cblb siRNA #1 and siRNA #2. Scale bar=50 μ m. Data are represented as mean \pm SD. Cbl mRNA level in nontransfected PC12 cells and PC12 cells transfected with scramble sequence, Cbl siRNA #1, siRNA #2, and siRNA #3 as detected by QRT-PCR (D). Data are represented as mean \pm SD. Quantitative analysis (E) and representative images (F) of cell neurite growth in NGF-stimulated PC12 cells transfected with scramble sequence, Cbl siRNA #1 and siRNA #2. Scale bar=50 μ m. Data are represented as mean \pm SD. NGF, neuronal growth factor; QRT-PCR, quantitative real-time polymerase chain reaction.

Additional file 11. Overexpression of Cblb and Cbl in PC12 cells. (A) Quantitative analysis of Cblb mRNA expression by QRT-PCR (B) and representative western blot images of Cblb. (C) Quantitative analysis of Cbl mRNA expression by QRT-PCR (B) and representative western blot images of Cbl. Data are represented as mean \pm SD. QRT-PCR, quantitative real-time polymerase chain reaction; EGFP, enhanced green fluorescent protein.

Additional file 12. Track of PKH26-labelled exosomes in vivo by confocal microscope. The nucleus (blue), Neu-N (green) and PKH26 (red and indicated by the red arrow) were stained to identify the uptake of exosomes by the injured neurons.

Additional file 13. Exosomal 199a-3p/145-5p strongly reduced inflammation levels. Representative western blot images (A) and quantitative analysis of IL-1 (B), IL-6 (C) and TNF- α (D). Data are represented as mean \pm SD.

Abbreviations

SCI: Spinal cord injury; LPS: Lipopolysaccharide; hUC-MSC: Human umbilical cord mesenchymal stem cell; EV: Extracellular vesicles; NGF: Neuronal growth factor; SNT: Suc-associated neurotrophic factor-induced tyrosine-phosphorylated target; FGF: Fibroblast growth factor; EGF: Epidermal growth factor; PDGF: Platelet-derived growth factor; MSC-Exo: MSC exosomes; SD: Standard difference; TPM: Transcripts per million; Exo-K: Exosomes with the inhibition of miR199a-3p/145-5p; PC12 cell: (rat) Pheochromocytoma cell; RT-QPCR: Quantitative real-time polymerase chain reaction; RAR β : Retinoic acid receptor β ; MAG: Myelin-associated glycoprotein; PLP: Proteolipid protein; PTEN1: Phosphatase and tensin homolog pseudogene; circRNAs: Circular ribonucleic acids; IFN: Interferon; G-CSF: Granulocyte-colony stimulating factor; MCP-1 α : Monocyte chemoattractant protein 1 α ; RTK: Receptor tyrosine kinase; MVBs: Multi-vesicular bodies; EGFR: Epidermal growth factor receptor; TRAF6: Tumor necrosis factor receptor-associated factor 6; SH2B2: src homology 2 adapter protein 2; NSAIDs: Non-steroidal anti-inflammatory drugs; PEG: Polyethylene glycol

Acknowledgements

We are so grateful for Zhenxiang Chen's and Yang Yang's contributions to constructing the SCI model of rats.

Authors' contributions

Conceptualization, LM R and Y W; Methodology, Y W, XW L, and DP W; Investigation, Y W, XW L, and DP W; Software, Y W and NX W; Formal analysis, Y W and DP W; Writing—original draft, Y W and NX W; Writing—review & editing, LM R and B L; Funding acquisition, LM R; Resources, LM R; Supervision, LM R and B L. The authors read and approved the final manuscript.

Funding

This work was supported by the National Key Research and Development Program of China (grant number 2017YFA0105403); the Key Research and Development Program of Guangdong Province (grant number 2019B020236002); the Clinical Innovation Research Program of Guangzhou Regenerative Medicine and Health Guangdong Laboratory (grant number 2018GZR0201006); the National Natural Science Foundation of China (grant numbers 31470949, 81772349); the Guangzhou Health Care Cooperative Innovation Major Project (grant number 201704020221); the Guangzhou Science and Technology Project (grant number 201707010115); the Guangdong Natural Science Foundation (grant number 2017A030313594); and the Medical Scientific Research Foundation of Guangdong Province (grant number A2018547).

Availability of data and materials

Not applicable.

Ethics approval and consent to participate

Not applicable.

Consent for publication

Not applicable.

Competing interests

No conflicts of interest are declared by all authors.

Author details

¹Department of Spine Surgery, The Third Affiliated Hospital of Sun Yat-sen University, No. 600 Tianhe Road, Tianhe District, Guangzhou, Guangdong Province, China. ²Guangdong Provincial Center for Engineering and Technology Research of Minimally Invasive Spine Surgery, No. 600 Tianhe Road, Tianhe District, Guangzhou, Guangdong Province, China. ³Guangdong Provincial Center for Quality Control of Minimally Invasive Spine Surgery, No. 600 Tianhe Road, Tianhe District, Guangzhou, Guangdong Province, China.

Received: 24 November 2020 Accepted: 6 January 2021

Published online: 12 February 2021

References

- Thompson C, Mutch J, Parent S. The changing demographics of traumatic spinal cord injury: an 11-year study of 831 patients. *J Spinal Cord Med.* 2015; 38(2):214–23.
- Taoka Y, Okajima K, Uchiba M. Role of neutrophils in spinal cord injury in the rat. *Neuroscience.* 1997;79(4):1177–82.
- Sandler AN, Tator CH. Effect of acute spinal cord compression injury on regional spinal cord blood flow in primates. *J Neurosurg.* 1976;45(6):660–76.
- Ahuja CS, Nori S, Tetreault L. Traumatic spinal cord injury-repair and regeneration. *Neurosurgery.* 2017;80(3S):S9–S22.
- Penney J, Tsai LH. JAKMIP1: translating the message for social behavior. *Neuron.* 2015;88(6):1070–2.
- Wutte C, Klein B, Becker J. Earlier decompression (< 8 hours) results in better neurological and functional outcome after traumatic thoracolumbar spinal cord injury. *J Neurotraum.* 2019;36(12):2020–7.
- Vafa Rahimi-Movaghar, Amin Niakan, Ali Haghnegahdar, Abtin Shahlaee, Soheil Saadat, Ehsan Barzideh. Early versus late surgical decompression for traumatic thoracic/thoracolumbar (T1-L1) spinal cord injured patients. Primary results of a randomized controlled trial at one year followup. *Neurosciences (Riyadh).* 2014;19(3):183–91.
- O Shea TM, Burda JE, Sofroniew MV. Cell biology of spinal cord injury and repair. *J Clin Invest.* 2017;127(9):3259–70.
- Pierotti MA, Greco A. Oncogenic rearrangements of the NTRK1/NGF receptor. *Cancer Lett.* 2006;232(1):90–8.
- Azmi AS, Bao B, Sarkar FH. Exosomes in cancer development, metastasis, and drug resistance: a comprehensive review. *Cancer Metastasis Rev.* 2013; 32(3–4):623–42.
- Tofaris GK. A critical assessment of exosomes in the pathogenesis and stratification of Parkinson's disease. *J Parkinsons Dis.* 2017;7(4):569–76.
- Zhang B, Yin Y, Lai RC. Mesenchymal stem cells secrete immunologically active exosomes. *Stem Cells Dev.* 2014;23(11):1233–44.
- Liu W, Wang Y, Gong F. Exosomes derived from bone mesenchymal stem cells repair traumatic spinal cord injury by suppressing the activation of A1 neurotoxic reactive astrocytes. *J Neurotraum.* 2019;36(3):469–84.
- Sun G, Li G, Li D. hucMSC derived exosomes promote functional recovery in spinal cord injury mice via attenuating inflammation. *Mater Sci Eng C.* 2018; 89:194–204.
- Zhang T, Liu C, Chi L. Suppression of miR-10a-5p in bone marrow mesenchymal stem cells enhances the therapeutic effect on spinal cord injury via BDNF. *Neurosci Lett.* 2020;714:134562.
- Saliminejad K, Khorram KH, Soleymani FS. An overview of microRNAs: biology, functions, therapeutics, and analysis methods. *J Cell Physiol.* 2019; 234(5):5451–65.
- Bhaskaran M, Mohan M. MicroRNAs: history, biogenesis, and their evolving role in animal development and disease. *Vet Pathol.* 2014;51(4):759–74.
- Fang S, Xu C, Zhang Y. Umbilical cord-derived mesenchymal stem cell-derived exosomal microRNAs suppress myofibroblast differentiation by inhibiting the transforming growth factor- β /SMAD2 pathway during wound healing. *Stem Cells Transl Med.* 2016;5(10):1425–39.
- Ma S, Zhang C, Zhang Z. Geniposide protects PC12 cells from lipopolysaccharide-evoked inflammatory injury via up-regulation of miR-145-5p. *Artif Cells Nanomed Biotechnol.* 2019;47(1):2875–81.
- Liddel SA, Guttenplan KA, Clarke LE. Neurotoxic reactive astrocytes are induced by activated microglia. *Nature.* 2017;541(7638):481–7.
- Jiang X, Shen Z, Chen J. Irisin protects against motor dysfunction of rats with spinal cord injury via adenosine 5'-monophosphate (AMP)-activated protein kinase-nuclear factor kappa-B pathway. *Front Pharmacol.* 2020;11: 582484.
- Ettenberg SA, Magnifico A, Cuello M. Cbl-b-dependent coordinated degradation of the epidermal growth factor receptor signaling complex. *J Biol Chem.* 2001;276(29):27677–84.
- Elly C, Witte S, Zhang Z. Tyrosine phosphorylation and complex formation of Cbl-b upon T cell receptor stimulation. *Oncogene.* 1999;18(5):1147–56.
- Ettenberg SA, Keane MM, Nau MM. Cbl-b inhibits epidermal growth factor receptor signaling. *Oncogene.* 1999;18(10):1855–66.
- Zhang J, Bárdos T, Li D. Cutting edge: regulation of T cell activation threshold by CD28 costimulation through targeting Cbl-b for ubiquitination. *J Immunol.* 2002;169(5):2236–40.
- Arévalo JC, Waite J, Rajagopal R. Cell survival through Trk neurotrophin receptors is differentially regulated by ubiquitination. *Neuron.* 2006;50(4): 549–59.
- Geetha T, Jiang J, Wooten MW. Lysine 63 polyubiquitination of the nerve growth factor receptor TrkA directs internalization and signaling. *Mol Cell.* 2005;20(2):301–12.
- Lagadec C, Meignan S, Adriaenssens E. TrkA overexpression enhances growth and metastasis of breast cancer cells. *Oncogene.* 2009;28(18):1960–70.
- Rong H, Jiao H, Hao Y. CD14 gene silencing alters the microRNA expression profile of RAW264.7 cells stimulated by *Brucella melitensis* infection. *Innate Immun.* 2017;23(5):424–31.
- Emdal KB, Pedersen A, Bekker-Jensen DB. Temporal proteomics of NGF-TrkA signaling identifies an inhibitory role for the E3 ligase Cbl-b in neuroblastoma cell differentiation. *Sci Signal.* 2015;8(374):a40.
- Qian X, Riccio A, Zhang Y. Identification and characterization of novel substrates of Trk receptors in developing neurons. *Neuron.* 1998;21(5):1017–29.
- Kwon BK, Okon E, Hillyer J. A systematic review of non-invasive pharmacologic neuroprotective treatments for acute spinal cord injury. *J Neurotrauma.* 2011; 28(8):1545–88.

Publisher's Note

Springer Nature remains neutral with regard to jurisdictional claims in published maps and institutional affiliations.